Is Any Free Flight/Wind Tunnel Equivalence Concept Valid for Unsteady Viscous Flow?

L. E. Ericsson*
Lockheed Missiles & Space Company, Inc., Sunnyvale, California

An analysis is presented showing that the present practice of using a free flight/wind tunnel equivalence concept derived for steady flow will not correctly simulate the unsteady flow effects when estimating the impact of dynamic stall on the performance of axial flow compressors and helicopter rotors. Furthermore, not even a free flight/wind tunnel equivalence concept derived for unsteady inviscid flow will correctly simulate the dynamic stall characteristics because of the unsteady viscous boundary condition at the airfoil surface, the so-called moving wall effect.

Nomenclature

c = chord length
f = frequency
k = frequency parameter, $k=\bar{\omega}/2$
K_a = dynamic overshoot parameter, Eqs. (7-10)
l = sectional lift; coefficients $c_l = l/(\rho_\infty U_\infty^2/2)c$, $\bar{c}_l$ = time-averaged value
m_p = sectional pitching moment, coefficient $c_m = m_p/(\rho_\infty U_\infty^2/2)c^2$
n = sectional normal force, coefficient $c_n = n/(\rho_\infty U_\infty^2/2)c$
p = static pressure
P = stagnation pressure
Re = Reynolds number based on chord length, $Re = U_\infty c/\nu_\infty$
t = time
U = horizontal velocity
V = resultant velocity, $V=\sqrt{V_A^2+V_\Omega^2}=U_\infty$
V_A = axial velocity
V_Ω = tangential velocity
W = vertical velocity
x = chordwise distance from the leading edge
z = translatory coordinate, positive downward
α = angle of attack
$\bar{\alpha}$ = equivalent angular amplitude, $\bar{\alpha} = |\dot{z}|/U_\infty$
α_0 = mean (trim) angle of attack
Δ = increment or amplitude
θ = perturbation in pitch
ξ = dimensionless x coordinate, $\xi = x/c$
ρ = air density
ν = kinematic viscosity
ψ = azimuth (Fig. 2)
ω = angular frequency, $\omega = 2\pi f$
$\bar{\omega}$ = reduced frequency, $\bar{\omega} = \omega c/U_\infty = 2k$

Subscripts

CG = center of gravity or rotation axis
e = boundary-layer edge
g = geometrically equivalent
G = gust
LE = leading edge
MAX = maximum
MIN = minimum
P = plunging
s = separation
w = wall
1,2 = numbering subscripts
∞ = freestream conditions

Derivative Symbols

$c_{l\alpha}$ = $\partial c_l/\partial\alpha$
$\dot{\alpha}$ = $\partial\alpha/\partial t$

Introduction

ONE of the great challenges facing the design engineer is how to use wind tunnel test data to assess the impact of dynamic stall on the performance of axial flow compressors and helicopter rotors. The standard procedure used to date has been to identify the instantaneous blade angle of attack and its rate of change and to use wind tunnel test results for a pitching airfoil to estimate the effects of dynamic stall. Examples of this type of analysis[1-3] are examined in light of more recent detailed investigations of dynamic stall[4-15] to determine to what extent the full-scale unsteady flow characteristics have been represented. It is found that this approach to dynamic simulation is too crude and that the classic free flight/wind tunnel equivalence concept remains valid only for steady flow. Further analysis shows that even the inviscid unsteady free flight/wind tunnel equivalence concept is invalid when considering unsteady separated flow characteristics.

Discussion

In an axial flow compressor,[1] the nonuniform inlet velocity distribution (Fig. 1a) generates a circumferentially varying instantaneous angle of attack at the compressor blade (Fig. 1b). In transforming the actual velocity vector geometry in Fig. 1a to be represented by the geometric angle of attack α_g and the total relative velocity vector V, all of the characteristics for stationary flow are preserved. In the case of a helicopter rotor, the axial velocity V_A in Fig. 1a is represented by the blade component U_∞ sin ψ of the forward speed of the helicopter. Adding to the sinusoidal α_g variation obtained in this manner is the effect of the downwash from the preceding blades(s), generating an instantaneous resultant angle-of-attack variation such as the one[2] shown in Fig. 2. For high forward speeds, this angle of attack can become larger than 90 deg for the retreating blade.[3] By adding the local time rate of change, $\dot{\alpha}c/U_\infty = \bar{\omega}\alpha$ ($\bar{\omega}=2k$ in Fig. 3) to the local instantaneous angle of attack, means are created for the use of experimental dynamic stall results for a pitching airfoil[1,3] (Fig. 4) to predict the time rate of change of the blade loading on an axial flow compressor[1] or a helicopter rotor.[2,3] Even when disregarding complex three-dimensional flow effects and the usual problem

Presented as Paper 85-0378 at the AIAA 23rd Aerospace Sciences Meeting, Reno, NV, Jan. 14-17, 1985; received Jan 31, 1985; revision received June 18, 1985.

*Senior Consulting Engineer, Fellow AIAA.

of Reynolds number scaling,[16] this approach to dynamic simulation is found to be highly questionable.

Analysis

The pressure gradient of the external flow at the boundary-layer edge is given by the Bernoulli equation for unsteady flow,

$$-\frac{1}{\rho_e}\frac{\partial p_e}{\partial x}=\frac{\partial U_e}{\partial t}+U_e\frac{\partial U_e}{\partial x} \tag{1}$$

or, with $\xi = x/c$,

$$\frac{\partial p_e}{\partial \xi}=-\rho_e U_e\left(\frac{\partial U_e}{\partial t}\frac{c}{U_e}+\frac{\partial U_e}{\partial \xi}\right) \tag{2}$$

That is,

$$\frac{\partial p_e}{\partial \xi}=\left(\frac{\partial p_e}{\partial \xi}\right)_{\dot{U}_e=0}-c\rho_e\frac{\partial U_e}{\partial t} \tag{3}$$

Equation (3) shows that the adversity of the pressure gradient $dp_e/d\xi$ will be decreased by an accelerating external velocity, $\partial U_e/\partial t > 0$. Thus, the separation on the leeward side of an airfoil will be delayed in an accelerating freestream. Conversely, separation will be promoted in a decelerating freestream.

For an airfoil pitching in a constant velocity freestream, the leeside flow acceleration is induced by the change of angle of attack,

$$\frac{\partial U_e}{\partial t}=\left(\frac{\partial U_e}{\partial \alpha}\right)\left(\frac{\partial \alpha}{\partial t}\right) \tag{4}$$

Thus, Eq. (2) can be written as follows for the pitching airfoil:

$$\frac{\partial p_e}{\partial \xi}=\left(\frac{\partial p_e}{\partial \xi}\right)_{\dot{\alpha}=0}+\frac{\partial p_e}{\partial \alpha}\frac{c\dot{\alpha}}{U_e} \tag{5}$$

The accelerated flow effect $(\partial p_e/\partial\alpha)(c\dot{\alpha}/U_e)$, where $\partial p_e/\partial \alpha < 0$, permits a dynamic overshoot of the static adverse pressure gradient, $(\partial p_e/\partial\xi)\dot{\alpha}=0$, before separation occurs, as has been discussed in detail elsewhere.[5,17,18]

Thus, on a pitching airfoil, the flow is accelerated on the leeward side when the angle of attack increases. In the case of axial flow compressors[1] and helicopter rotors,[2,3] the increase of the local angle of attack is associated with decelerating freestream flow and, consequently, decelerating leeside flow on the airfoil. The importance of this difference is examined below.

The acceleration-induced separation delay on the pitching airfoil gives a corresponding overshoot of static $c_{l\,\max}$,[5]

$$\Delta c_{l\,\max}=c_{l\alpha}\Delta\alpha_{s1} \tag{6}$$

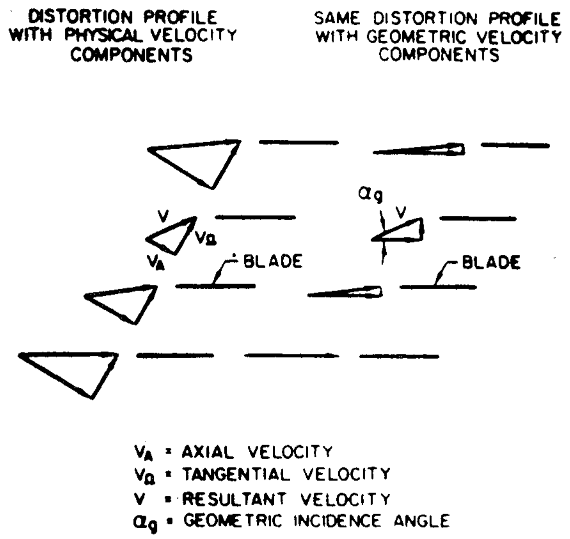

a) Typical axial velocity distortion.

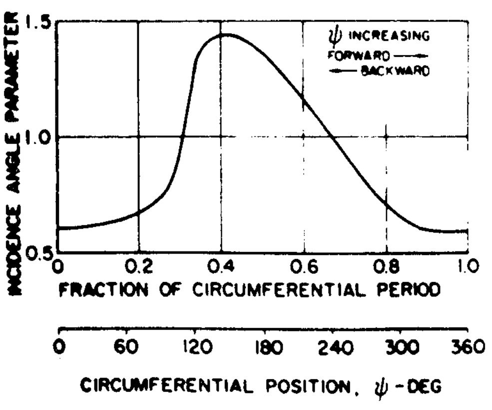

b) Hypothetical distortion profile.

Fig. 1 Dynamic stall analysis of axial flow compressor (Ref. 1).

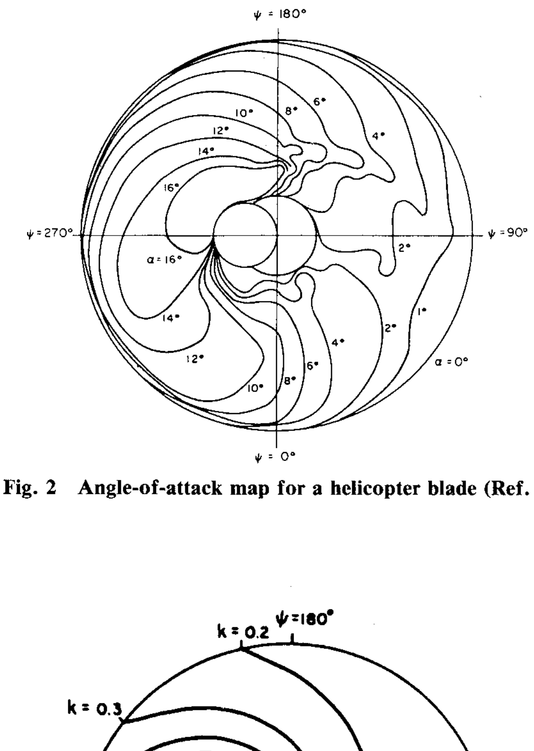

Fig. 2 Angle-of-attack map for a helicopter blade (Ref. 2).

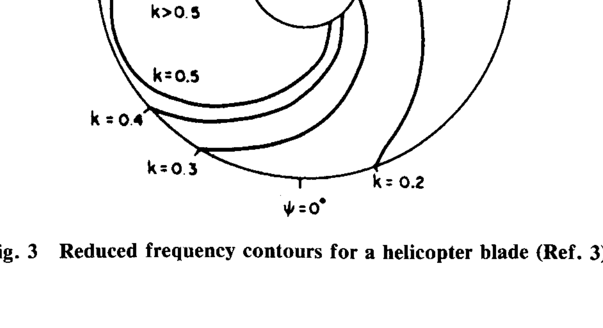

Fig. 3 Reduced frequency contours for a helicopter blade (Ref. 3).

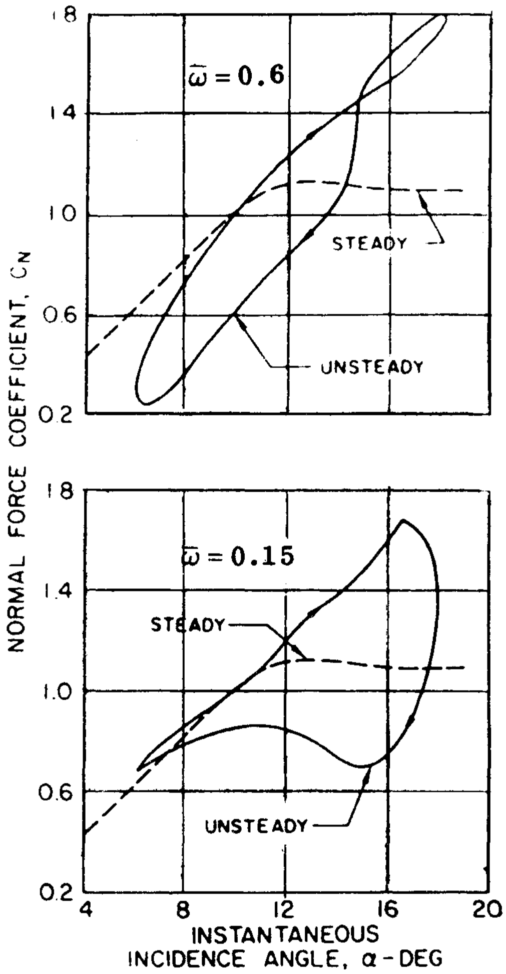

Fig. 4 Dynamic stall characteristics of NACA-0012 (Ref. 1).

$$\Delta\alpha_{s1} = K_{a1}\frac{c\dot{\alpha}}{U_e} \tag{7}$$

Another mechanism for dynamic overshoot of static $c_{l\,max}$ by a pitching airfoil is the so-called "leading-edge-jet" effect.[5,18] See Fig. 5. It causes an overshoot $c_{l\alpha}\Delta\alpha_{s2}$ of static $c_{l\,max}$, which in a first approximation is proportional to the leading-edge plunging velocity

$$\Delta\alpha_{s2} = -K_{a2}(\dot{z}_{LE}/U) \tag{8}$$

Thus, combining Eqs. (7) and (8) one obtains for the airfoil pitching around the center of gravity,

$$\Delta\alpha_s = K_a c\dot{\alpha}/U_e \tag{9}$$

$$K_a = K_{a1} + K_{a2}\xi_{CG} \tag{10}$$

Equations (6) and (9) forecast an undershoot of static $c_{l\,max}$ when the airfoil decreases angle of attack on the pitching "downstroke." Recent experimental results[7] (Fig. 6) support this forecast and indicate that the effects of decelerating leeside flow on dynamic stall are as adverse as the accelerating flow effects are favorable.

Experimental results[19] indicate that an accelerating free-stream can generate large overshoot of static $c_{l\,max}$ (Fig. 7). An equally large overshoot is generated by accelerating the airfoil in longitudinal oscillations[11] (Fig. 8). The figure shows the time-averaged lift $\bar{c}_l(t)$ obtained for the complete pitch loop around α_0 (See Fig. 4 for loop examples.) The reason $c_l(t)$ increases with increasing $\bar{\omega}$ and associated increasing $|U_\infty c/U_\infty^2|$ is that a leading-edge vortex is spilled near the end of the

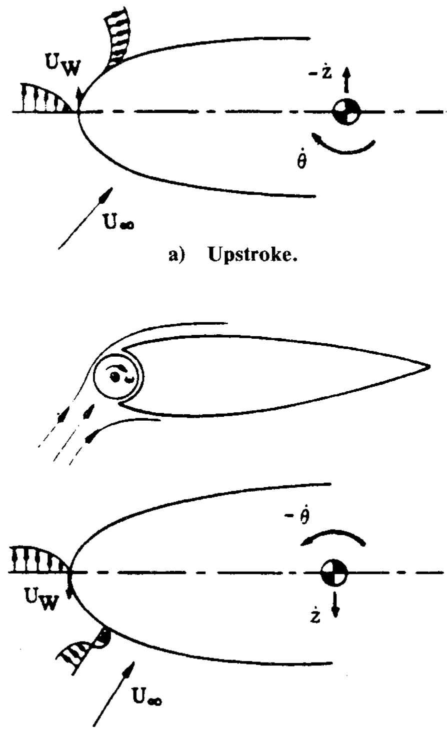

a) Upstroke.

b) Downstroke.

Fig. 5 "Leading edge jet" effect.

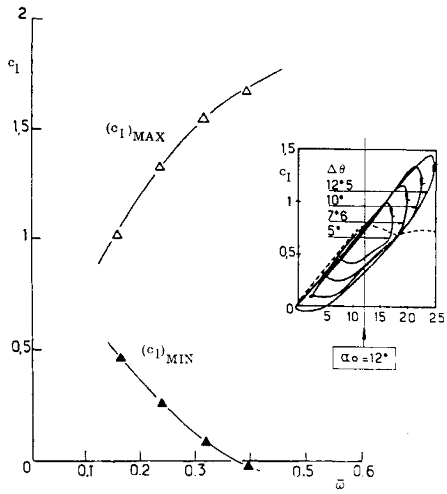

Fig. 6 Effect of reduced frequency on maximum and minimum lift (Ref. 7).

upstroke, generating lift during its travel from the leading to trailing edge during the pitching downstroke.[20] When $\bar{\omega} > 0.656$, the flow will reattach at the leading edge before the "spilled" vortex passes downstream of the trailing edge.[18] This explains the overshoot of the extrapolated attached flow lift for $\bar{\omega} = 0.656$, 0.926, and 1.314 in Fig. 8. Replotting the results against $\dot{U}c/U_\infty^2 = \bar{\omega}^2\Delta x/c$ gives a data trend[13] in agreement with that in Fig. 7, when considering the difference between time-averaged and instantaneous lift just discussed (Fig. 9).

Free Flight/Wind Tunnel Equivalence

It is clear from the results shown in Figs. 7-9 that the free flight/wind tunnel equivalence concept derived for stationary flow cannot be applied to unsteady flow. However, the results show that the effect of accelerating the airfoil in a constant-

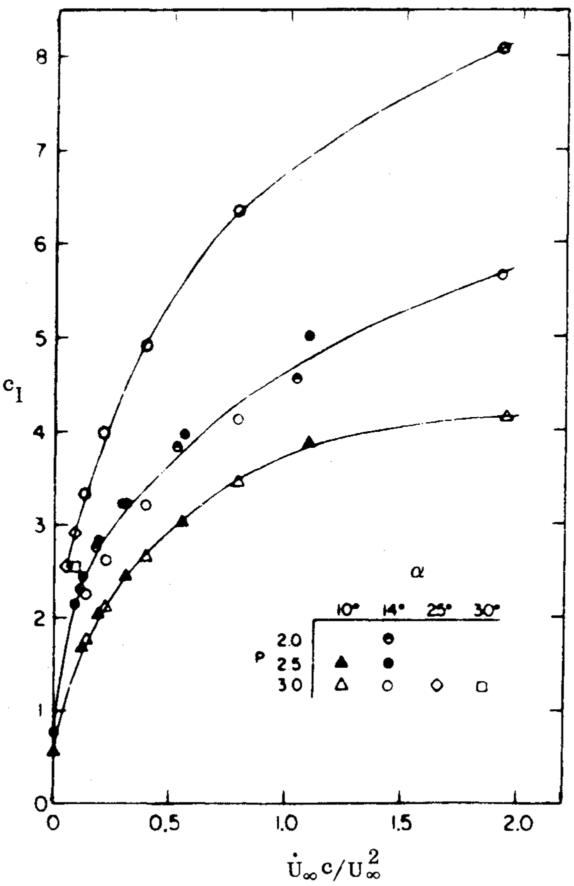

Fig. 7 Effect of flow acceleration on the lift of NACA-0015 (Ref. 19).

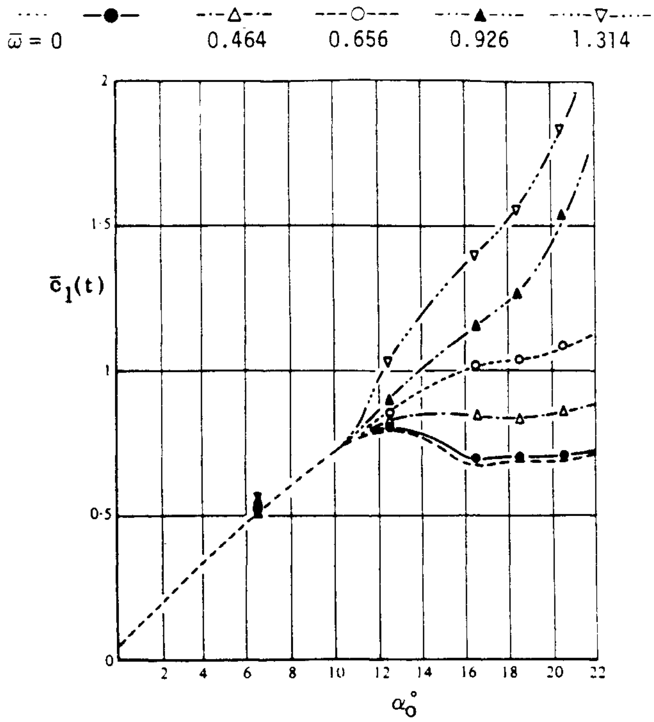

Fig. 8 Time-averaged lift for streamwise airfoil oscillation of amplitude $\Delta x/c = 0.565$ (Ref. 11).

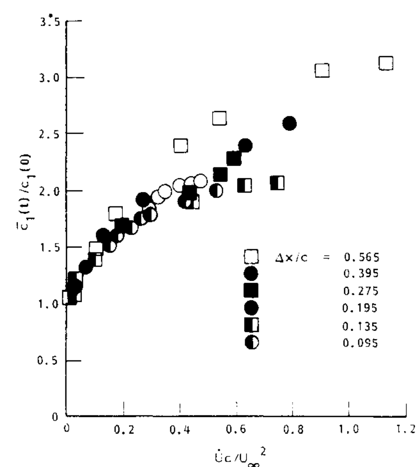

Fig. 9 Effect of normalized acceleration parameter on time-averaged lift (Ref. 18).

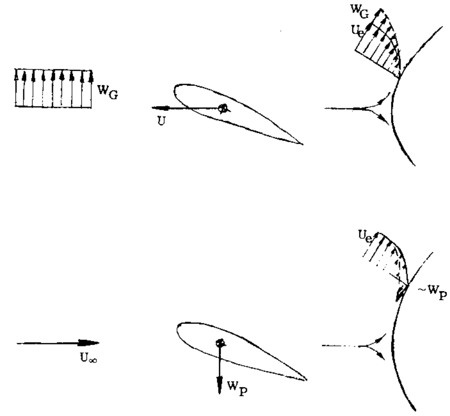

Fig. 10 Nonequivalence between gust encounter and airfoil plunging.

velocity stream is equivalent to accelerating the stream over a stationary airfoil. Thus, for inviscid flow effects, such as the boundary-layer edge conditions discussed earlier, the free flight/wind tunnel equivalence concept derived for unsteady flow is valid. The next question is: can this inviscid unsteady flow equivalence concept be applied to viscous flow effects, in particular those associated with separated flow? The answer is "no," as is shown below.

The "leading-edge jet" or "moving wall" effect illustrated in Fig. 5 is the reason for the "no" answer (Fig. 10). In the free flight case, the encounter of a vertical gust W_G will cause this velocity component to be added to the boundary-layer edge velocity in the nose region of an airfoil. In contrast, in the wind tunnel, imposing a sudden plunging velocity W_P to the airfoil section will add the velocity component, not at the boundary-layer edge but at the airfoil surface. Thus, the perturbation effect on dynamic stall will be opposite in the two cases. In the free flight case, the increased boundary-layer edge velocity will delay flow separation, whereas the upstream moving wall effect in the wind tunnel test will promote separation, as has been discussed (downstroke in Fig. 5). As any unsteady event can be represented in form of a series of stepwise changes, the general conclusion to be drawn is that, in the case of unsteady viscous flow, the unsteady flow equivalence between airfoil motion and freestream oscillation is not valid.

The so-called moving wall effect is of significant magnitude only in the nose flow region where the boundary layer is thin.[5,18,21] That is, of course, why lateral or vertical translation generates large moving wall effects (Fig. 5). In contrast, longitudinal or horizontal oscillations will not generate significant moving wall velocities in the nose flow region. This is the reason the inviscid unsteady equivalence concept is supported by the viscous experimental results in Figs. 7-9.

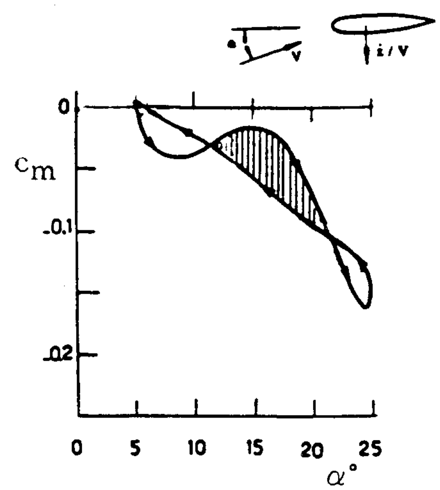

a) Plunging.

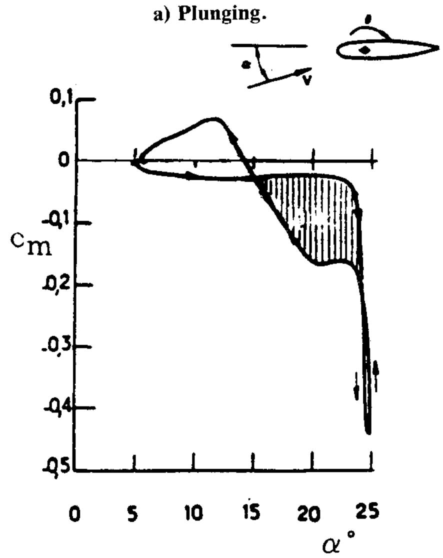

b) Pitching.

Fig. 11 Moment loops for plunging and pitching oscillations of the NACA-0012 airfoil.

Some appreciation of the effect of the different unsteady boundary-layer profiles shown in Fig. 10 can be obtained by comparing the dynamic stall results for pitching and plunging airfoils for which the moving wall effects are opposite (Fig. 5), i.e., delaying stall for a pitching airfoil (during the upstroke) and promoting stall for a plunging airfoil, which increases its $\bar{\alpha}$ during the downstroke rather than during the upstroke. The experimental results obtained by Maresca, Favier, and Rebont[6] show dynamic stall† to occur at $\alpha \approx 16$ deg for the plunging airfoil (Fig. 11a) compared to the delay of stall to $\alpha \approx 24$ deg measured for a pitching airfoil[22] (Fig. 11b). This agrees with the expectations expressed earlier and illustrates the problem addressed in the present paper, if one lets the pitching airfoil represent the case of the gust encouter (Fig. 10a).

Conclusions

An analysis of existing experimental results for dynamic airfoil stall has led to the following conclusions:

1) The free flight/wind tunnel equivalence concept derived for stationary flow conditions cannot be applied to inviscid or viscous unsteady flow analysis, as is presently standard practice.

2) The free flight/wind tunnel equivalence concept derived for unsteady inviscid flow in general, cannot be applied to dynamic stall analysis because of the unsteady viscous boundary condition at the airfoil surface, the so-called moving wall effect.

†The loss of the leading-edge suction at stall results in a corresponding loss of pitching moment, amplified by the "spilled" vortex effect.[20]

References

[1]Carta, F. O., "Unsteady Normal Force on an Airfoil in a Periodically Stalled Inlet Flow," *Journal of Aircraft,* Vol. 4, Sept.-Oct. 1967, pp. 416-421.

[2]Ham, N. D., "Helicopter Blade Flutter," AGARD Rept. 607, Jan. 1973.

[3]Carta, F. O., "An Analysis of the Stall Flutter Instability of Helicopter Rotor Blades," with comment by N. D. Ham, "Stall Flutter of Helicopter Rotor Blades—Special Case of the Dynamic Stall Phenomenon," Paper presented at Annual Forum of the American Helicopter Society, Washington, D. C., May 1967.

[4]McCroskey, W. J., "The Phenomenon of Dynamic Stall," NASA TM 81264, March 1981, (also *VKI Lecture Series,* No. 1981-4, paper 2).

[5]Ericsson, L. E. and Reding, J. P., "Dynamic Stall Analysis in Light of Recent Numerical and Experimental Results," *Journal of Aircraft,* Vol. 13, April 1976, pp. 248-255.

[6]Maresca, C. A., Favier, D. J., and Rebont, J. M., 'Unsteady Aerodynamics of an Airfoil at High Angle of Incidence Performing Various Linear Oscillations in a Uniform Stream," *Journal of the American Helicopter Society,* April 1981, pp. 40-45.

[7]Favier, D., Rebont, J., and Maresca, C., "Profil d'Aile a Grande Incidence Animé d'un Mouvement de Pilonnement," 16éme Colloque d'Aerodynamique Appliquée, Lille, France, Nov. 1979.

[8]Carta, F. O., "A Comparison of the Pitching and Plunging Response of an Oscillating Airfoil," NASA CR 3172, Oct. 1979.

[9]McCroskey, W. J., Carr, L. W., and McAlister, K. W., "Dynamic Stall Experiments on Oscillating Airfoils," *AIAA Journal,* Vol. 14, Jan. 1976, pp. 57-63.

[10]McCroskey, W. J., McAlister, K. W., Carr, L. W., Pucci, S. L., Lambert, O., and Indergrand, R. F., "Dynamic Stall on Advanced Airfoil Sections," *Journal of the American Helicopter Society,* July 1981, pp. 40-50.

[11]Maresca, C. A., Favier, D. J., and Rebont, J. M., "Experiments on an Airfoil at High Angle of Incidence in Longitudinal Oscillations," *Journal of Fluid Mechanics,* Vol. 92, Pt. 4, 1979, pp. 671-690.

[12]Maresca, C., Rebont, J., and Valensi, J., "Separation and Reattachment of the Boundary Layer on a Symmetric Airfoil Oscillating at a Fixed Incidence in Steady Flow," *Proceedings of University of Arizona/USAFOSR Symposium on Unsteady Aerodynamics,* edited by R. B. Kinney, University of Arizona Press, Tucson, 1975, pp. 35-54.

[13]Carta, F. O., "Analysis of Oscillatory Pressure Data Including Dynamic Stall Effects," NASA CR-2394, May 1974.

[14]McAlister, K. W., Carr, L. W., and McCroskey, W. J., "Dynamic Stall Experiments on the NACA 0012 Airfoil," NASA TP 1100, Jan. 1978.

[15]McCroskey, W. J., McAlister, K. W., Carr, L. W., and Pucci, S. L., "An Experimental Study of Dynamic Stall on Advanced Airfoil Sections, Vol. 1, Summary of the Experiment," NASA TM 84245, July 1982.

[16]Ericsson, L. E. and Reding, J. P., "How to Cope with the Problem of Scaling and Support Interference in Dynamic Subscale Tests," AIAA Paper 84-0382, Jan. 1984.

[17]Ericsson, L. E. and Reding, J. P., "Unsteady Airfoil Stall, Review and Extension," *Journal of Aircraft,* Vol. 8, Aug. 1971, pp. 609-616.

[18]Ericsson, L. E. and Reding, J. P., "Unsteady Flow Concepts for Dynamic Stall Analysis," *Journal of Aircraft,* Vol. 21, Aug. 1984, pp. 601-606.

[19]Minkkinen, G. T., Wilson, Ta. A., and Beavers, G. S., "An Experiment on the Lift of an Accelerated Airfoil," *AIAA Journal,* Vol. 14, May 1976, pp 687-689.

[20]Ericsson, L. E. and Reding, J. P., "Dynamic Stall at High Frequency and Large Amplitude," *Journal of Aircraft,* Vol. 17, March 1980, pp. 136-142.

[21]Ericsson, L. E. and Reding, J. P., "Analytic Prediction of Dynamic Stall Characteristics," AIAA Paper 72-682, June 1972.

[22]Carr, L. W., McAlister, K. W., and McCroskey, W. J., "Analysis of Development of Dynamic Stall Based on Oscillation Airfoil Experiments," NASA TN D8382, 1977.